JOURNAL OF MATERIALS SCIENCE 16 (1981) 84–94

Simulated strength–grain size study using a glass–glass-ceramic composite system

ANIL V. VIRKAR
Department of Materials Science and Engineering, University of Utah, Salt Lake City, Utah 84112, USA

Strength studies have been conducted on composite specimens of a glass and a glass-ceramic. The composite system consists of a glass fillet on the surface of a bar-shaped glass-ceramic. Controlled surface flaws have been introduced into the glass fillet via indentation. Strength has been studied as a function of indent load and the size of the glass fillet. The glass–glass-ceramic composite system is meant to represent a polycrystalline ceramic with duplex microstructure such that the glass fillet simulates a large single crystal. The glass-ceramic on the other hand simulates a fine-grained matrix. Thus, the present study simulates a strength versus grain size relation for a polycrystalline ceramic. The data indicate that in several coarse grained ceramics, an inherent crack arrests within the body after initial propagation prior to catastrophic failure. Microscopic examination coupled with an electric potential method indicated that the initial crack arrests at the glass–glass-ceramic interface. The data also suggests that differences in elastic constants across an interface may have a significant influence on strength.

1. Introduction

Of all the mechanical properties of ceramics, strength is probably the most widely studied. To date, literally hundreds of studies have addressed the subject of strength of ceramics as it relates to microstructure, processing variables, methods of testing etc. With regard to the dependence of strength on microstructure two specific parameters are of interest, namely the grain size and porosity. Several studies [1–7] have shown that, typically, strength decreases with increasing grain size. Strength data are generally plotted versus $1/\sqrt{D}$ where D is the grain size. The probable origin of this methodology lies in the early attempts to relate strength to grain size via a relation similar to the Hall–Petch relation in metals [8]. Strength, σ_F versus $1/\sqrt{D}$ plots are often bimodal with two linear branches. At large grain sizes the slope is generally quite steep while at small grain sizes the strength is weakly dependent on grain size. Often, the data can be fitted to a single straight line [7]. The intercept can be non-zero although in several cases the line passes through the origin.

The bimodal nature of σ_F versus $1/\sqrt{D}$ plots was originally explained by Carniglia [9] on the basis of microplastic effects. A similar explanation was given by Rice [7]. However, later work by Rice [10] indicated that the bimodal nature of the σ_F versus $1/\sqrt{D}$ plots in ceramics is primarily due to the fact that single-crystal fracture energy γ_S, is smaller than polycrystalline fracture energy, γ_{eff}, and fractographic examination has shown that machine-induced flaws are approximately independent of grain size. Rice thus suggested that in fine-grained ceramics the inherent crack is larger than the grain size, $C > D$. Therefore, the strength of fine-grained bodies will be determined by C and γ_{eff} (or polycrystalline critical stress intensity factor K_{ICP}). In coarse-grained bodies, the inherent crack will be less than the grain size i.e. $C < D$. Rice therefore suggested that the strength should be determined by C and γ_S. The change in slope of σ_F versus $1/\sqrt{D}$ should occur at $C \approx D$ (according to Rice) and the slope in the large grain regime should correspond to the single-crystal fracture energy, γ_S.

Recently, Singh *et al.* [11] have examined energy balance of the growth of a microcrack in

0022–2461/81/010084–11$03.10/0

a material with spatially varying fracture energy. In this analysis it was assumed that the only energies involved in the process of fracture are strain, surface and kinetic. Furthermore, quasi-static approximation was used i.e. the shape of the deformed body under the conditions of rapid crack growth was assumed to be the same as that for the static case. This assumption has been made in the past by Mott [12], Berry [13] and Virkar and Johnson [14]. The analysis by Singh *et al.* [11] shows that a small crack contained within a single grain would extend under the application of load followed by an arrest within the polycrystalline region in the majority of cases of interest. A subsequent increment in load would be required to completely fracture the body. Thus, the failure stress would be determined by K_{ICP} and not by K_{ICS} (the single-crystal critical stress intensity factor) as suggested by Rice. Also, the steep slope on the σ_F versus $1/\sqrt{D}$ plot may correspond to the polycrystalline fracture energy, γ_{eff}, and not single-crystal fracture energy, γ_S. Furthermore, the initial propagation and arrest of an inherent crack prior to catastrophic failure cannot be detected in a typical strength test where a specimen is continuously loaded to failure since the change in compliance is negligibly small.

The objective of the present work was to investigate the concept of crack arrest in materials with large-grained microstructure. In view of the fact that it is difficult to control the location of the initiation of failure, the size of the grain in which failure initiates and the size of the inherent flaw, a simulation system which represents a material with duplex microstructure was designed in the present study. The system chosen consists of a glass-ceramic specimen with a surface groove filled with glass. The glass fillet represents a large surface grain which becomes the failure initiating size. The dimension of the fillet represents the size of the large grain. Furthermore, a microcrack of controlled size can be introduced into the glass fillet by indentation. The fracture energies of the glass and the glass-ceramic can be independently determined. Thus, one has a complete knowledge of the initial crack C_0, the grain size D (i.e. the fillet size or the groove depth), the γ_S (fracture surface energy of the glass) and γ_{eff} (fracture surface energy of the glass-ceramic). Thus it should be possible to study the dependence of strength on these parameters. The results of such a study should simulate the strength–grain size relationship in materials with duplex microstructure i.e. materials containing a few large grains in a matrix of fine grains. The choice of duplex materials for the analogy is used for the following reasons. (1) Several materials of technological interest exhibit duplex microstructure e.g. β-alumina, SiC. (2) In large structures of ceramic materials of otherwise uniform microstructure, the probability of the existence of inclusions, second-phase particles cannot be entirely eliminated. Failure often initiates from such inhomogeneities. (3) The above discussed simulation can be achieved with relative ease to represent materials with duplex microstructure.

2. Experimental procedure

2.1. Materials

Appropriate choice of materials is particularly important so that a realistic simulation of a material with duplex microstructure is achieved. The properties of interest are (1) elastic properties (2) coefficients of thermal expansion and (3) fracture properties. The elastic and thermal properties of the glass and the glass-ceramic should be closely matched but the fracture toughness of the glass-ceramic must be significantly greater than that of the glass which represents a large single crystal on the surface. Furthermore, the glass should exhibit excellent bonding with the glass-ceramic.

A machinable glass-ceramic* was used to represent the fine-grained matrix while low melting lead glasses† were used to represent the single crystals. Fig. 1 shows a micrograph of Macor. The relevant information on the physical and mechanical properties is given in Table I. As can be seen, the glass 7570 and Macor are well matched with respect to the coefficient of thermal expansion while glass 8463 has a somewhat higher coefficient of thermal expansion. The Young's elastic moduli of both of the glasses are somewhat lower than that of Macor with 8463 showing larger deviation. It should be emphasized, however, that such differences are to be expected in most polycrystalline materials with duplex microstructures since the elastic and thermal properties of most single crystals vary significantly with orientation. Low melting lead glasses were chosen so that the grooves could be filled at low temperatures with-

*Macor by Corning.
†No. 7570 and 8463 by Corning.

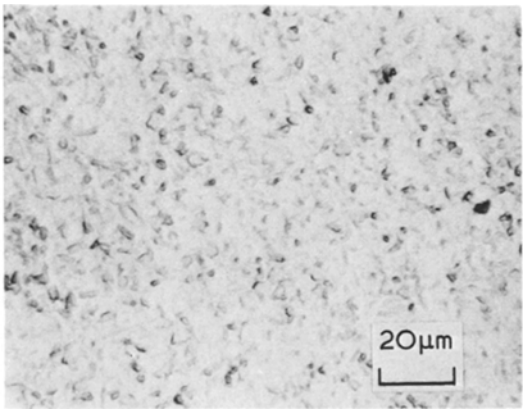

Figure 1 An optical micrograph of Macor. The specimen was polished on an 0.3 μm alumina wheel and a thin layer of gold was vapour deposited.

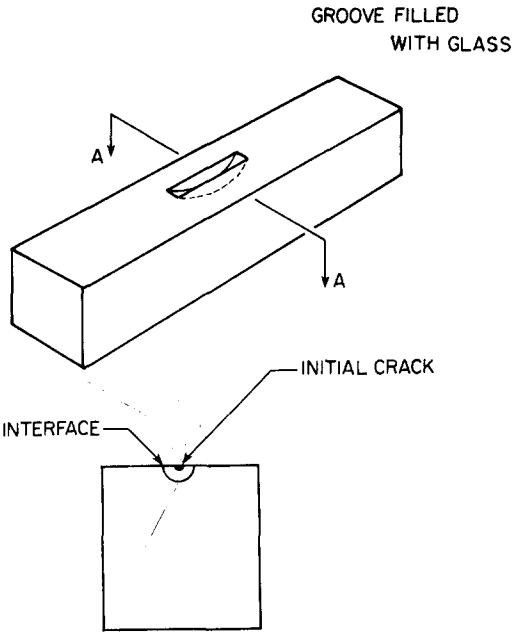

Figure 2 A schematic diagram showing the specimen geometry. The grooves are made longitudinally using diamond blades of various thicknesses.

out causing any change in the microstructure of the glass ceramic. The K_{IC} of Macor was determined using a double cantilever beam technique. The K_{IC} of glasses were not determined but are expected to be $\approx 0.7 \times 10^6\ N\,m^{-3/2}$ typical of most glasses.

2.2. Specimen preparation

Rectangular beam specimens of dimensions 5 mm x 5 mm x 4.5 cm were cut from large billets using a diamond blade. Surface grooves of various widths and depths were machined longitudinally using diamond blades of thickness varying from 0.05 to 1.0 mm. The specimens were subsequently annealed at 925° C for 1/2 h to minimize machining damage in the form of microcracks which may have been introduced at the root of the grooves. The grooves were filled with a thick paste of glass powder (7570 or 8463) made with acetone. The specimens were then heated in a furnace to a temperature of 650° C to fuse the glass into the grooves. The resulting glass fillets were generally bubble-free. The specimens were ground and metallographically polished on a 0.3 μm alumina polishing wheel. The specimens were then annealed above the annealing point of the glass in order to relieve any residual stresses followed by a slow furnace cool.

Controlled surface flaws were introduced into the glass fillets using a Knoop indentor in such a way that the long axis of the indentor was perpendicular to the axis of the specimens. This technique of introducing controlled surface flaws has been previously used successfully by several researchers [15–17]. Sharp cracks were seen to emanate from the indent along the long axis. The specimens were further annealed for 1 h above the strain point of the glass to relieve any stresses introduced by indentation. Fig. 2 shows a schematic diagram of the specimen used.

TABLE I Physical and mechanical properties of the glass and the glass-ceramic

Glass or glass-ceramic	Young's modulus (psi)	K_{IC} ($N\,m^{-3/2}$)	Coefficient of thermal expansion ($^\circ C^{-1}$)	Setting point (° C)
Macor	9.3×10^6	1.4×10^6	9.4×10^{-6} up to 400° C	1100
7570 glass	8.0×10^6	ND	9.2×10^{-6} up to 347° C	347
8463 glass	7.51×10^6	ND	10.5×10^{-6} up to 310° C	310

ND – Not determined.

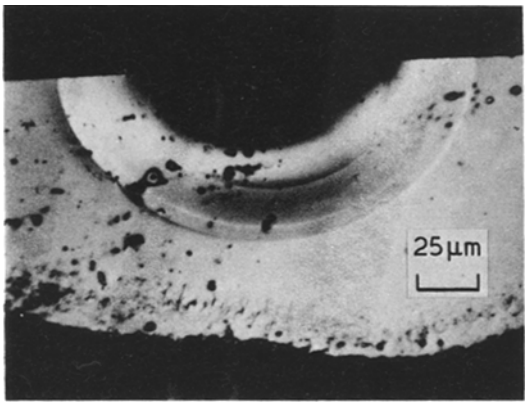

Figure 3 A typical semicircular flaw introduced into glass fillets using Knoop hardness indentation. The photomicrograph was taken after breaking the specimens in bending.

2.3. Strength testing

The specimens were broken in four-point bending under a cross-head speed of 0.125 mm min^{-1} on a universal testing machine.* The inner load point span was 9.375 mm and the outer one was 31.25 mm. Some of the specimens were broken in air while others were first ovendried and then coated with vacuum grease prior to testing for strength. The vacuum grease used had negligible solubility for water. Thus, moisture assisted subcritical crack growth was essentially eliminated. Strength testing was conducted with varying sizes of the glass fillets as well as various indent loads.

For larger fillet sizes (groove depths ≈ 0.5 mm), the groove depth was a significant portion of the thickness of the specimens. Thus, the calculated strengths were multiplied by a correction factor, $f = (1 - 2D/\pi T)$ where D is the groove depth and T the thickness of the specimen. This correction factor was calculated by taking the varying stress field from the surface into the bulk in bending into account. The indentation technique yielded a nearly semicircular flaw as shown in Fig. 3.

3. Results

3.1. Strength as a function of indent load

Fig. 4 shows a plot of strength versus indent load for specimens with two different groove sizes (glass fillet sizes) for both 7570 and 8463 glasses. Strength data shown in this figure were obtained in air without vacuum grease coating. It is easily seen that strength for a given groove size (fillet size) is independent of the indent load over the range of indent loads used in the present experiments. Microscopic examination indicated that the size of the surface flaw introduced by indentation was approximately linearly related to the indent load. Thus, Fig. 4 shows that the strength was independent of the initial flaw size even though the failure in every case initiated at the indent. The strength, however, was dependent upon the fillet size; strength decreased with increasing fillet size. It was also noted that the strength of 8463-Macor

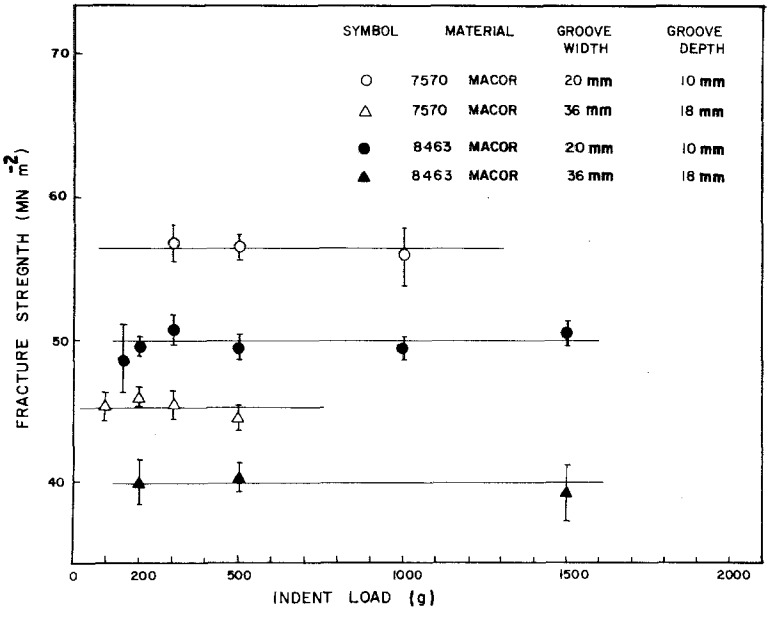

Figure 4 Strength versus indent load plot for 7t70-Macor and 8463-Macor specimens for two different groove dimensions. The strength is independent of indent load but depends upon groove dimension. The strength of 7570-Macor specimens is consistently higher than that of 8463-Macor for the same groove dimension.

*Instron Corporation, Canton, Massachusetts, USA.

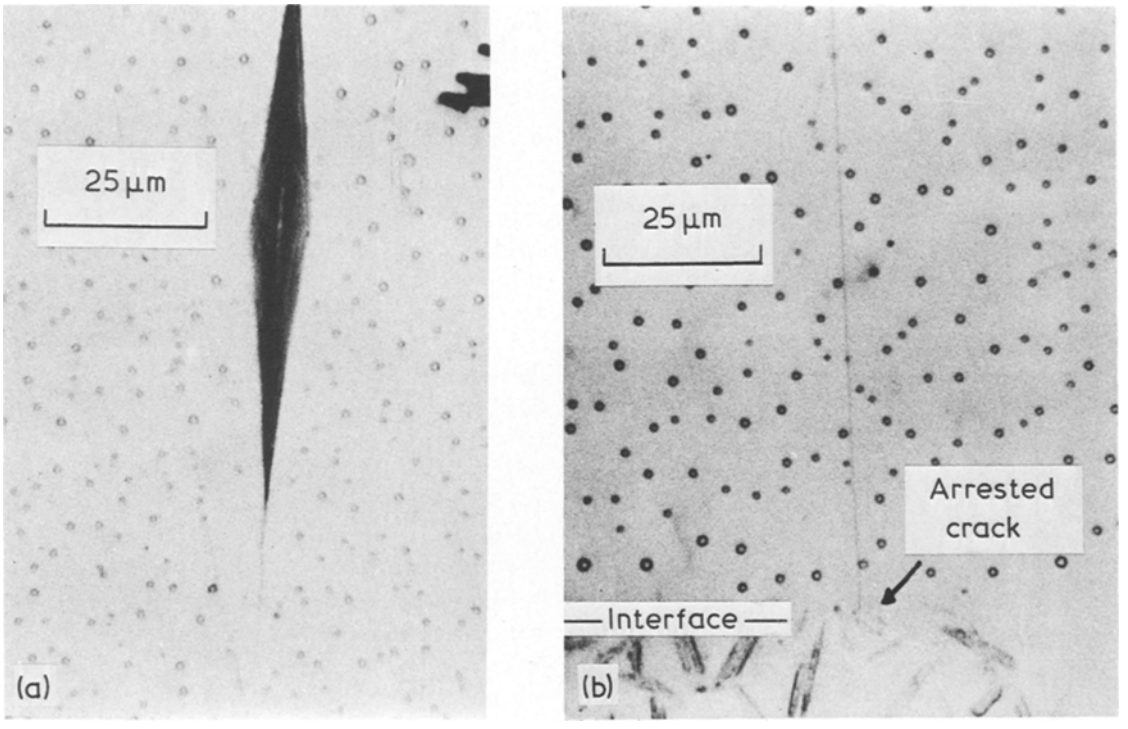

Figure 5 (a) A photomicrograph showing the Knoop indent with sharp cracks emanating from the sharp corners. Gold has been sputtered onto the specimen to enhance reflectivity. The circular features are not pores, but some artifacts. (b) A photomicrograph showing crack arrest at the glass–Macor interface. This specimen was loaded to 8.9 kg and unloaded. The crack arrested right at the interface. Part of the picture near the interface is out of focus because of a step formation caused by preferential polishing of the glass.

specimens was consistently lower than 7570-Macor for identical fillet sizes. For indent loads below 100 g, often the failure did not occur at the indent and the strength was higher with more specimen to specimen scatter.

The lack of dependence of strength on the initial flaw size but dependence on the fillet size indicates that the original flaw was not the critical flaw. It must have grown and arrested near the glass–glass-ceramic interface prior to catastrophic failure. To explore the possibility of crack arrest, some of the specimens were subjected to increasing loads followed by unloading for microscopic examination. It was observed that the initial flaw in the glass (shown in Fig. 5a) was essentially unchanged in size up to a certain load. When the specimens were subjected to loads past this critical load, the crack rapidly propagated and arrested at the glass–glass-ceramic interface (Fig. 5b). This initial propagation and arrest was not detectable on load–deflection charts as is to be expected since the flaw size is much smaller than the specimen size [11]. The lack of dependence of strength on the initial flaw size can now be understood to be due to the fact that the initial flaw propagated and arrested prior to failure.

3.2. Strength as a function of groove depth

7570-Macor and 8463-Macor specimens of various groove depths (fillet sizes) were tested for strength in the same manner as discussed earlier. Strength tests were conducted in air with and without vacuum grease coating. The specimens were typically indented with a 500 g load prior to strength tests. Based on the strength data and K_{IC} of Macor,* the size of the critical flaw was calculated assuming that the flaw shape was always semicircular. The flaw size is then given by [16]

$$C_F = 0.74\left(\frac{K_{IC}}{\sigma_F}\right)^2. \quad (1)$$

*K_{IC} of Macor was determined using a DCB test. Eight specimens were used which yielded an average value for K_{IC} of $1.4 \times 10^6\,N\,m^{-3/2}$.

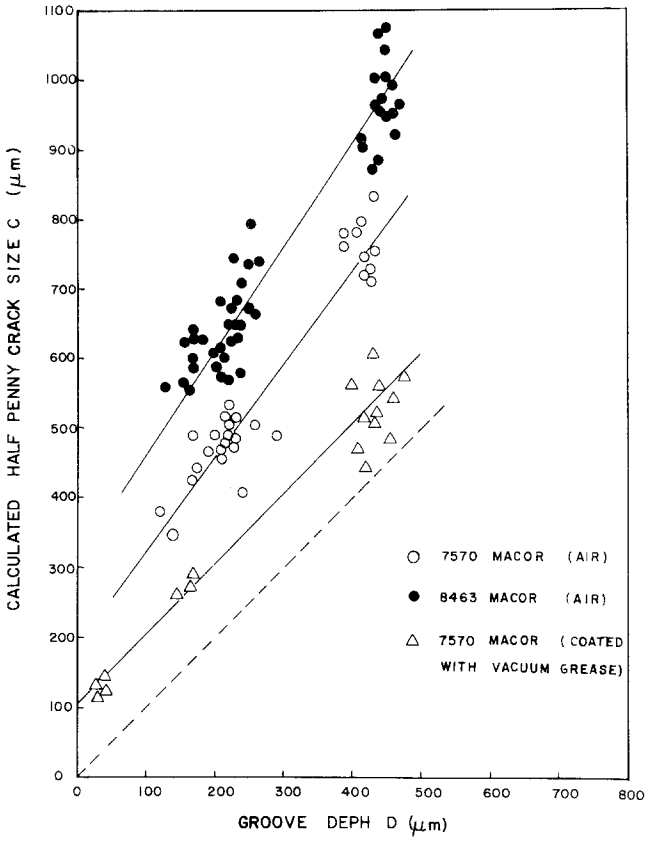

Figure 6 Calculated flaw size (from strength and K_{IC}) versus groove depth plots for 7570-Macor and 8463-Macor. The dotted line is drawn for $C = D$.

The calculated flaw sizes (radii) are plotted versus the groove depth in Fig. 6. The data points shown are for individual specimens. This approach was chosen since the groove sizes, as measured under a microscope after fracturing, generally varied slightly from specimen to specimen. The variation was generally within a few microns. Only a few representative data points are shown in the figure in order to prevent overlap.

As can be seen, the flaw size increases with increasing groove depth. The 7570-Macor specimens tested in air without vacuum grease coating exhibit higher crack size for any given groove depth compared with the specimens which were coated with vacuum grease. This difference is clearly due to environment assisted crack growth. Also, the C versus D line for specimens without vacuum grease coating exhibits a greater slope; i.e. the amount of slow crack growth (ΔC) increases with increasing groove depth ("initial" arrested crack size).

The dotted line in Fig. 6 is drawn for $C = D$. The specimens coated with vacuum grease, however, yield crack sizes that are about 100 μm larger than the corresponding groove depth. Furthermore, the 8463-Macor specimens exhibit larger C values than the corresponding 7570-Macor specimens. The probable explanation is presented in the discussion section.

As the groove depth (or glass fillet dimension) is meant to represent a large surface grain in a polycrystalline ceramic, the strength σ_F may be plotted versus $1/\sqrt{D}$ as is the usual practice. Strength versus $10^3/\sqrt{D}$ is plotted for 7570-Macor specimens in Fig. 7. The data can be fitted very well with straight lines for both the specimens coated with vacuum grease and the uncoated specimens. The dotted line represents the predicted σ_F versus $10^3/\sqrt{D}$ plot for $C = D$ i.e. the slope of the line corresponds to K_{IC} of Macor (simulated polycrystalline K_{IC}). The data, although fitted to a straight line, clearly deviates significantly from it. Furthermore, the intercept is non zero. The slope of the line (7570-Macor, with vacuum grease coating) corresponds to 0.55×10^6 N m$^{-3/2}$.

3.3. Independent check on crack arrest

An independent check on the propagation and arrest of the initial crack in the glass fillet was obtained by using the electrical potential tech-

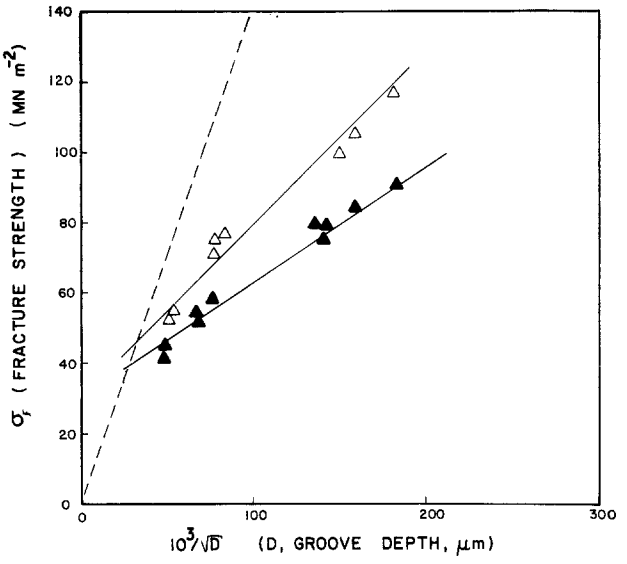

Figure 7 Strength σ_F versus $10^3/\sqrt{D}$ for 7570-Macor specimens. The open triangles are for specimens tested with vacuum grease coating. The filled triangles show the data for specimens tested without vacuum grease coating. Both sets of data can be fitted to straight lines with non zero intercepts. The dotted line corresponds to $C = D$ and K_{IC} of Macor.

nique [18]. A part of the specimen surface was masked using a tape and a thin layer of gold was vapour deposited. Electrical contacts were made to the gold film by wrapping two copper wires and coating with silver paint as shown in Fig. 8. A Knoop indentation was introduced within the glass fillet. A small d.c. current (100 μA) was passed through the gold film using a constant current d.c. power supply and the voltage drop was recorded on a strip chart recorder. The specimen was then subjected to bending in a universal testing machine. Typical voltage versus time traces obtained are shown schematically in Fig. 9. In the majority of cases, the voltage versus time curves were of the type shown in Fig. 9a. The voltage was seen to remain nearly constant for some time (point A in the figure) followed by an abrupt rise in voltage to point B. Specimens unloaded immediately after the abrupt rise in voltage showed that the initial crack had extended all the way to the glass–glass-ceramic interface. Further loading resulted in a smooth continuous rise in voltage indicative of subcritical crack growth in Macor.

Occasionally, the voltage versus time curve resembled the one shown in Fig. 9b in which an abrupt rise in voltage, of smaller magnitudes, occurred at two different times. If the indent produces a crack at only one of the sharp corners, then only part of the crack runs all the way to the interface at some load and the remaining crack front extends to the interface only after further increase in load. Such behaviour yields a curve of the type shown in Fig. 9b. If the rate of loading is extremely slow, the voltage versus time curve resembles the one shown in Fig. 9c which arises due to slow crack growth in both the glass

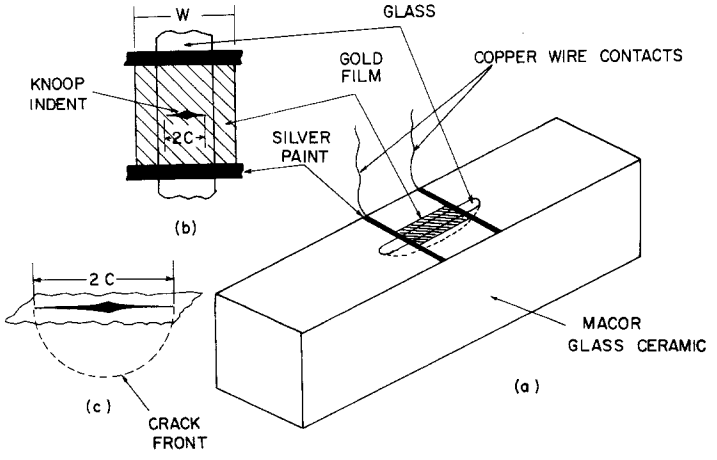

Figure 8 (a) A schematic diagram showing a glass–Macor composite specimen with a thin film of gold (vapour deposited) which partly covers the glass and Macor. (b) The shaded area is the gold film. A sharp crack is introduced via a Knoop indentation. (c) The dotted semicircle shows a schematic diagram of the crack front.

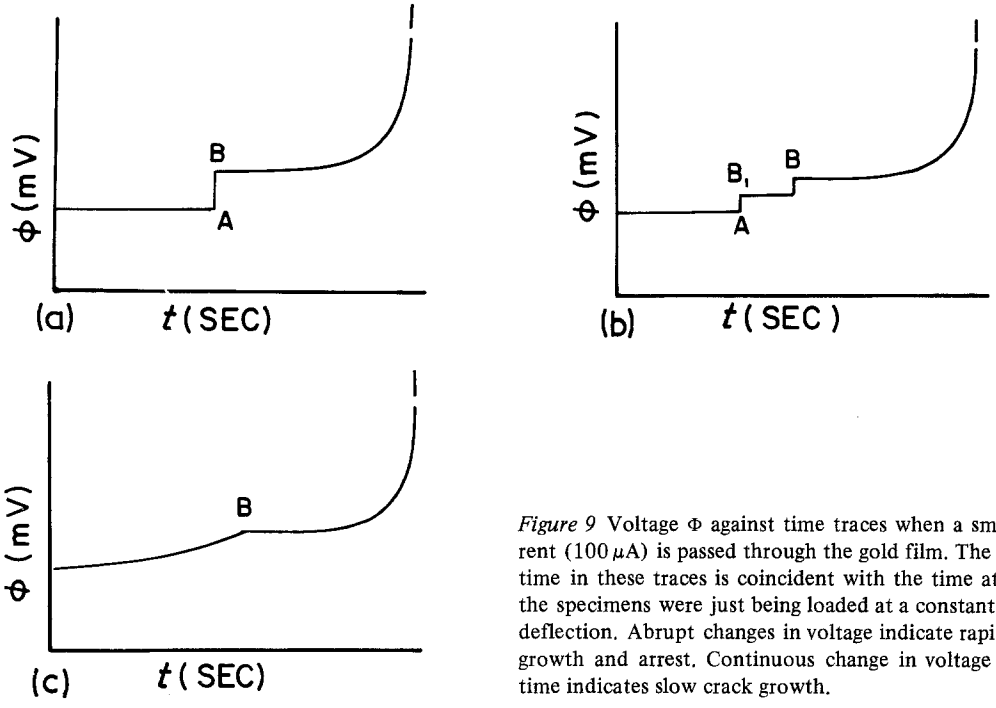

Figure 9 Voltage Φ against time traces when a small current (100 μA) is passed through the gold film. The zero of time in these traces is coincident with the time at which the specimens were just being loaded at a constant rate of deflection. Abrupt changes in voltage indicate rapid crack growth and arrest. Continuous change in voltage against time indicates slow crack growth.

and the glass-ceramic. These experiments further confirmed the concept of crack arrest at the interface.

4. Discussion

The present experiments have shown that for the range of groove (glass fillet) depths and the range of indent loads used, the strength of the glass–glass-ceramic composites was independent of the load or the initial crack size. Thus, the initial crack must have arrested near the glass–glass-ceramic interface after initial propagation prior to catastrophic failure. Direct microscopic examination after subjecting to increasing loads as well as the electrical potential technique confirmed that the crack arrest did indeed take place. Furthermore, it was also found that the crack arrest always took place right at the interface and that there was no overshoot of the crack into the glass-ceramic due to the kinetic energy of the propagating crack as proposed by Singh *et al.* [11]. Thus, the model by Singh *et al.* [11] yields an overestimation of the arrest crack length or a conservative estimate of the strength. The kinetic energy of the propagating crack (i.e. kinetic energy due to the material moving perpendicular to the direction of the propagation crack) is not converted to surface energy but is perhaps converted into acoustic energy. Based on the work of Eshelby [19], this is perhaps to be expected with regards to cracks that are much smaller than the specimen size. Specifically Eshelby [19] has shown that a crack tip could be regarded as a particle of zero mass. Thus, the velocity of a crack can change discontinuously. A crack, according to Eshelby, can begin to propagate with a finite velocity and a crack travelling with a finite velocity may come to halt discontinuously if it meets with resistance it cannot overcome. The present experiments do indeed indicate that the rapidly propagating cracks in the glass were suddenly arrested at the glass–glass-ceramic interface. The present conclusions with regards to the lack of overshoot are only for small cracks, since in the case of large cracks (with respect to the specimens size) there is sufficient time for the reflected waves to arrive back at the crack tip in the form of loading or unloading waves and crack overshoot can occur. This in fact has been observed [20].

The data on strength versus $10^3/\sqrt{D}$ can be fitted to a straight line as shown in Fig. 7. Experimental work clearly showed that the initial crack arrested at the interface prior to its further growth leading to catastrophic failure. The strength was therefore controlled by the K_{IC} of Macor. Even then the slope of the σ_F versus $10^3/\sqrt{D}$ line did not agree with K_{IC} of Macor (1.4×10^6 N m$^{-3/2}$) but corresponded to a value of 0.55×10^6 N m$^{-3/2}$.

Although K_{IC} for the glass has not yet been determined, it is expected to be about 0.7×10^6 N m$^{-3/2}$. As discussed earlier, the glass–glass-ceramic composite system here is meant to represent a material with duplex microstructure or a material containing large inclusions in a matrix of fine grained ceramic. Since in most ceramics, particularly large structures, it is often difficult, if not impossible, to obtain a completely uniform microstructure, the present composite system could conceivably describe failure characteristics of many ceramics. Consequently, an apparent agreement between the slope (σ_F versus $1/\sqrt{D}$) and single-crystal K_{ICS} or fracture energy does not imply that the strength is determined by single-crystal K_{ICS} as has been suggested by Rice [10]. This apparent agreement may be fortuitous. The present data, σ_F versus $10^3/\sqrt{D}$ also extrapolates to a non-zero intercept as has been observed in several other ceramics.

The existence of a considerably lower slope on the σ_F versus $10^3/\sqrt{D}$ plot even though the failure was controlled by the failure of Macor, warrants further discussion of this point. As shown in Fig. 6, for the 7570-Macor specimens tested with vacuum grease coating, the calculated flaw size is about 100 μm greater than the groove depth for all of the groove sizes studied. If the experimental determination of K_{IC} of Macor were not accurate the calculated flaw size versus groove depth plot would not be parallel to the $C = D$ plot (dotted line in Fig. 6). Thus, the K_{IC} measurement must be quite accurate. There are two possible reasons for the occurrence of an anomalously low slope on the σ_F versus $10^3/\sqrt{D}$ plot or discrepancy between the calculated flaw size and groove depth. Firstly, it is possible that at the root of the groove there are numerous microcracks of the order of 100 μm in depth. Thus, the original crack in the glass after having been propagated to the root of the groove may link up with the microcracks to yield a higher value of C than the groove depth D. The electrical potential technique however indicated that there was only one discrete jump in voltage (except in cases where the indentation did not produce cracks at both of the sharp corners on the indent) and that optical microscopy indicated that the discrete jump in voltage corresponded to crack propagation and arrest at the interface. It appears therefore that linking of microcracks with the main crack is perhaps not the reason. The other possibility is related to the perturbations in stress intensity factors that occur near an interface separating materials with differing elastic constants. Several researchers have investigated the nature of stress singularity and the perturbations in stress intensity factors in bimaterial plates [21–23]. Extensive analytical work in this area is largely due to Erdogan and co-workers [24–26]. Although to the authors knowledge no calculations exist for the three dimensional problems with surface semi-circular crack in a bimaterial configuration of the type used in the present experiments, it is to be expected that due to the singularity at the interface conventional stress intensity calculations or crack size calculations using K_{IC} data will have to be modified. This could be reflected as a discrepancy between the calculated flaw size and the glass fillet size with the resultant lower value of slope than expected on the σ_F versus $1/\sqrt{D}$ plot. In many ceramic materials with duplex microstructure a similar effect could take place. When a crack contained in a large grain extends across a grain boundary into the neighbouring fine grained matrix, the crack would see differences in elastic constants which are orientation dependent. This is illustrated schematically in Fig. 10. The 8463-Macor specimens consistently exhibited lower strength compared with the 7570-Macor specimens. This may also be related to the fact that

$$\frac{E_{\text{Macor}}}{E_{8463}} > \frac{E_{\text{Macor}}}{E_{7570}}.$$

Further, more definitive work which examines crack interactions at the interface is needed to fully explore the effect of differences in elastic constants on strength.

The present work which clearly demonstrates that the initial crack may propagate and arrest prior to leading to catastrophic failure has important implications with regards to proof testing procedure. Consider a material which has different stress corrosion susceptibility parameters for the single crystal and the polycrystal such that $N_S > N_P$ (where N represents the stress corrosion susceptibility parameter defined by the equation $V = AK_I^N$ where V is the crack velocity and A is a constant). This is possible if for example the material is fabricated using a glassy phase. Then, if the initial crack is contained within a single large grain and further crack propagation is intergrannular (through the glassy phase), N_S would in general be greater than N_P. If some of the specimens are prooftested at a stress level where

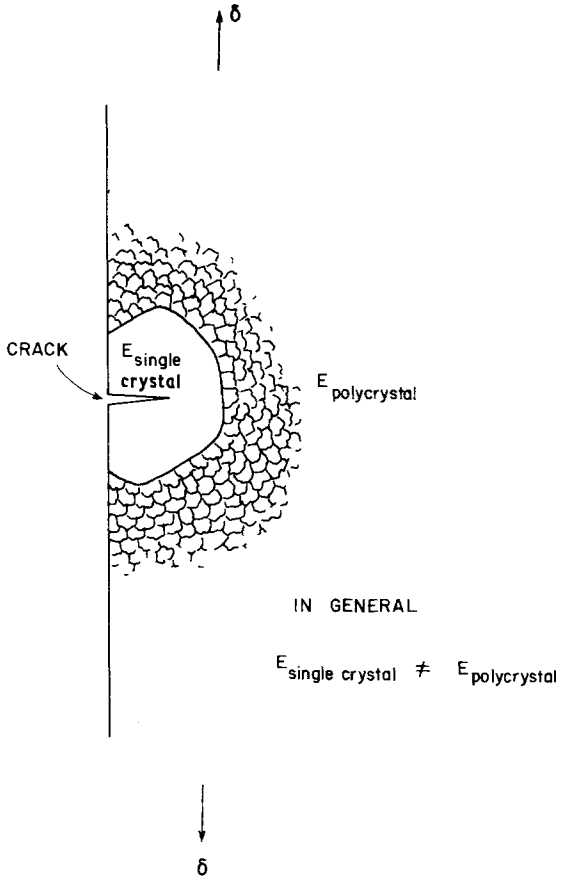

Figure 10 A schematic diagram showing a crack contained within a single large grain in a material with a duplex microstructure. The crack as it crosses the grain boundary region, will cross an interface across which the elastic moduli will in general be different. The conventional way of calculating K_I (or crack length using K_{IC} data) would be in error due to perturbations in K_I near the interface.

the initial crack propagates and arrests at the grain boundary and if some are not, it is to be expected that both groups of specimens would show identical inert strength. (It is assumed that no environment assisted crack growth occurred during prooftesting). One would therefore conclude that prooftesting has not damaged the specimens. If now both of the groups of specimens are subjected to static loads far below the proof stress, the failure times for the two groups in general will be different. In the prooftested specimens, the subcritical crack growth would occur only in the polycrystalline region given by N_P. On the other hand, in the specimens that were not prooftested, slow crack growth would first occur in the single-crystal region (controlled by N_S), and once the crack crosses the grain boundary, slow crack growth would occur controlled by N_P. Thus, in general, the specimens that are not prooftested could have a longer failure time. (This statement does not take into account statistical variation in strength. Or in other words, assumes a very high Weibull parameter, m). The larger the differences in N_S and N_P (with $N_S > N_P$) the larger will be the difference in failure times. Furthermore, the lower the load applied, the larger the difference in failure times. The above discussion demonstrates that there are situations where prooftesting could considerably damage structures even though no apparent damage is introduced during prooftesting.

5. Conclusions

Based on the present work, the following conclusions can be drawn.

(1) For the range of glass fillet sizes studied, an initial crack propagates and arrests prior to catastrophic failure. Thus, in several polycrystalline materials, the polycrystalline fracture energy would determine the strength and not the single crystal fracture energy even though the initial crack is smaller than the grain size.

(2) The arrest of the initial crack occurs at the interface and no overshoot of the crack was observed due to the kinetic energy. This may be either due to the dissipation of kinetic energy in forms other than surface energy or due to the perturbations in stress intensity factor near the interface separating materials with different elastic constants or both.

(3) Anomalously low values of the slope of strength versus $(\text{grain size})^{-1/2}$ plots does not imply that strength is controlled by single crystal fracture energy. This may be related to perturbations in stress intensity factor near the interface.

Acknowledgements

This work was supported by the National Science Foundation under grant No. DMR 76 04110.

References

1. F. P. KNUDSEN, *J. Amer. Ceram. Soc.* **42** (1959) 376.
2. R. M. SPRIGGS and T. VASILOS, *ibid.* **46** (1963) 224.
3. T. VASILOS, J. B. MITCHELL and R. M. SPRIGGS, *ibid.* **47** (1974) 606.
4. S. PROCHAZKA and R. J. CHARLES, in "Fracture Mechanics of Ceramics" Vol. 2, edited by R. C. Bradt, D. P. H. Hasselman and F. F. Lange (Plenum Press, New York, 1974) pp. 579–598.
5. A. V. VIRKAR and R. S. GORDON, *J. Amer. Ceram. Soc.* **60** (1977) 58.

6. D. C. CRANMER, R. E. TRESSLER and R. C. BRADT, *ibid.* **60** (1977) 230.
7. R. W. RICE, *Proc. Brit. Ceram. Soc.* **20** (1972) 205.
8. N. J. PETCH, *J. Iron Steel Inst.* **173** (1954) 25.
9. S. C. CARNIGLIA, *J. Amer. Ceram. Soc.* **48** (1965) 580.
10. R. W. RICE, in "Fracture Mechanics of Ceramics", Vol. 1, edited by R. C. Bradt, D. P. H. Hasselman and F. F. Lange, (Plenum Press, New York, 1974).
11. J. P. SINGH, A. V. VIRKAR, D. K. SHETTY and R. S. GORDON, *J. Amer. Ceram. Soc.* **62** (1979) 179.
12. N. F. MOTT, *Engineering* **16** (1948) 2.
13. J. P. BERRY, *J. Mech. Phys. Solids* **8** (1960) 207.
14. A. V. VIRKAR and D. L. JOHNSON, *J. Amer. Ceram. Soc.* **58** (1976) 197.
15. N. INGLESTRON and H. NORDBERG, *Eng. Fract. Mech.* **6** (1974) 597.
16. J. J. PETROVIC, L. A. JACOBSON, P. K. TALTY and A. K. VASUDEVAN, *J. Amer. Ceram. Soc.* **58** (1975) 113.
17. R. K. GOVILA, K. R. KINSMAN and P. BEARDMORE, *J. Mater. Sci.* **13** (1978) 2081.
18. A. V. VIRKAR, *J. Amer. Ceram. Soc.* **63** (1980) 219.
19. J. D. ESHELBY, *J. Mech Phys. Solids* **17** (1969) 177.
20. "Fast Fracture and Crack Arrest" edited by M. F. Kanninen and G. T. Hahn, ASTM-STP 627 (American Society for Testing Materials, Philadelphia, 1976).
21. R. K. LEVERENZ, *Int. J. Fract. Mech.* **8** (1972) 311.
22. K. Y. LIN and J. W. MAR, *Int. J. Fract.* **12** [4], 521 (1976).
23. J. TIROSH and A. S. TETELMAN, *ibid.* **12** (1976) 187.
24. T. S. COOK and F. ERDOGAN, *Int. J. Eng. Sci.* **10** (1972) 667.
25. F. ERDOGAN and V. BIRICIKOGLU, *ibid.* **11** (1973) 745.
26. F. ERDOGAN, *J. Appl. Mech.* **32** (1965) 403.

Received 12 July 1979 and accepted 22 May 1980.